AN ACCUMULATOR/PRE-BOOSTER FOR THE MEDIUM-ENERGY ELECTRON ION COLLIDER AT JLAB

B. Erdelyi[*,^], S. Manikonda[*], P. Ostroumov[*], S. Abeyratne[^], Y. Derbenev[#], G. Krafft[#], Y. Zhang[#]
[*]Physics Division, Argonne National Laboratory, Argonne, IL 60439
[^]Department of Physics, Northern Illinois University, DeKalb, IL 50115
[#]CASA, Thomas Jefferson National Accelerator Facility, Newport News, VA 23606

Abstract

Future nuclear physics facilities such as the proposed electron ion collider (MEIC) will need to achieve record high luminosities in order to maximize discovery potential. Among the necessary ingredients is the ability to generate, accumulate, accelerate, and store high current ion beams from protons to lead ions. One of the main components of this ion accelerator complex for MEIC chain is the accumulator that also doubles as a pre-booster, which takes 285MeV protons from a superconducting linear accelerator, accumulates on the order of 1A beam, and boosts its energy to 3GeV, before extraction to the next accelerator in the chain, the large booster. This paper describes its design concepts, and summarizes some preliminary results, including linear optics, space charge dynamics, and spin polarization resonance analysis.

INTRODUCTION

The pre-booster ring is an essential component of the ion accelerator complex, which will accept beam pulses of any ions from the preceding linear accelerator and after accumulation and/or acceleration will transfer the beam to the subsequent large booster for further acceleration. The layout of the MEIC facility [1] and the location of the pre-booster ring are shown in Figure 1. The exact mechanisms of pre-booster operation will depend on the ion species. The two extreme cases are polarized protons and un-polarized lead ion beams. In the following we describe briefly the similarities and distinctions of these two scenarios.

Protons: a pulse of around 0.22ms protons of 285MeV kinetic energy is injected in the ring utilizing multi-turn injection with combined longitudinal and transverse painting, using the charge exchange injection mechanism. The resulting coasting beam is captured and accelerated with the first harmonic up to 3GeV and fast-extracted to the large booster.

Heavy ions: a number of pulses of around 0.25ms of ions of approximately 100MeV/u kinetic energy are injected in the ring by the same multi-turn painting scheme as in the case of protons. However, the painted phase space region is smaller (about half the acceptance) in order to leave room for the stack. The stacking/accumulation are performed with the help of the drag-and-cool conventional DC electron cooling method. The method is repeated as necessary to reach the required beam intensity. The cooled stack is accelerated to approximately 670MeV/u on first harmonic and fast-extracted to the large booster.

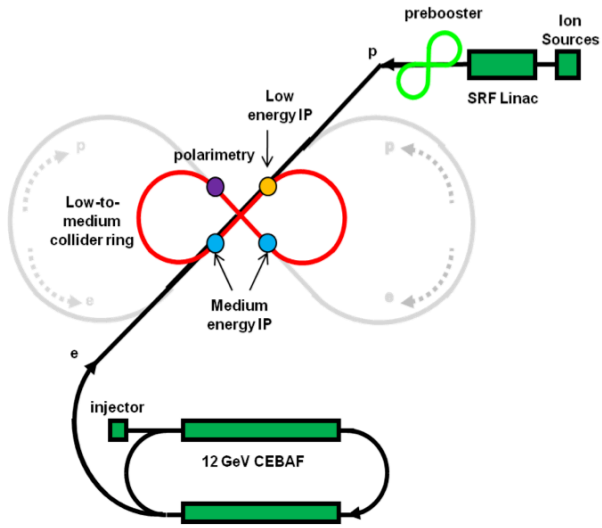

Figure 1: Schematic view of the MEIC facility showing the low-to-medium energy collider rings, ion sources, SRF Linac, prebooster and 12 GeV CEBAF. The faded ring is the future upgrade for MEIC.

OPTIMIZED DESIGN FOR THE PRE-BOOSTER RING

For the pre-booster ring a figure-8 shape was considered due to the ease of spin transport, manipulation and preservation [2]. The pre-booster design comprises of (quasi) independent module sections that can be optimized separately. The result of a series of design optimizations - the ring shown in Figure 2 - satisfies the properties and constraints mentioned above. The arc on the left hand side (ARC3) consist of 9 standard FODO cells with total phase advance being a multiple of 2π, making dispersion suppressors unnecessary at the arc's ends. The arc on the right hand side includes similar standard FODO cells (ARC1 & ARC2 containing three cells each) and a matched injection insert in between with an identity transfer matrix. The middle of the injection region contains a long straight with large constant normalized dispersion for efficient injection painting in all three phase planes simultaneously. The two main arcs are linked by two long straight sections composed of triplet cells. The triplet cells allow long drifts with round beam. Also, the long drifts allow the installation of several necessary components such as electron cooling devices, RF cavities, collimation, extraction regions, and

possibly further solenoids and other elements for horizontal-vertical decoupling. Finally, the straights are linked to the arcs by dedicated matching modules consisting of five quadrupoles. The role of these sections is to match the optics between straights and arcs and provide independent knobs for setting the tunes. Since the ellipses are upright by design at the ends of the matching sections, only two sets of settings are needed, the other two being the mirror symmetric versions of the first two. The optics corresponding to the outline shown in Fig. 2 is presented in Figure 3. The circumference is 234 m, and the horizontal, vertical tunes are (7.96, 6.79). Maximum beta functions are below 30 m, and the dispersion's absolute value is less than 3.4 m. The ring will always operate below transition. More details and magnet parameters needed to produce the optics shown in Figs. 2 and 3 are listed in Table 1.

Table 1: 234 m Pre-Booster Ring Lattice Parameters

Parameters	Units	Value
Total length	m	234
Angle at crossing	deg	75
Number of dispersive FODO cells (Type I)		6
Number of dispersive FODO cells (Type II)		9
Number of triplet cells		10
Number of matching cells		4
Minimum drift length between magnets	cm	50
Drift lengths in the insertion region	m	5.0
Drift lengths between triplets (RF, collimation and electron cooling)	m	5.0
Beta maximum in X	m	16
Beta maximum in Y	m	32
Maximum beam size	cm	2.3
Maximum beam size in the dipole magnets	cm	0.5
Maximum Dispersion ($x\mid \delta_p$)		3.36
Normalized dispersion at injection $(x\mid\delta_p)/\sqrt{\beta_x}$		2.53
Tune in X		7.96
Tune in Y		6.79
Gamma of particle (proton at 3 GeV)		4.22
Gamma at Transition Energy		5
Momentum compaction factor		0.04
Number of quadrupole Magnets		95
Quadrupole magnet Length	cm	40
Quadrupole magnet Half Aperture	cm	5
Quadrupole maximum pole tip field	T	1.53
Number of Dipoles		36
Dipole Vertical full gap	cm	3
Dipole Max Strength	T	1.41
Dipole Bending Radius	m	9
Dipole Angle	deg	≈14

Finally, the RF cavities used to form and accelerate the beams, together with the lattice, optics, and magnets used to inject, transport and extract the beams to the large booster produce the beam parameters contained in Table 2 for the case of protons, and Table 3 for the case of heavy ions. Uniform beam profile has been assumed for computation of acceptance and emittance values. The lead beam emittances after cooling have been set in order to limit the maximum Laslett tune shift to 0.3. This might require partial blow-up of transverse emittances after cooling. Another option is reducing the current requirements by accumulation in the large booster.

Table 2: Main Parameters of Proton Beams

Parameter	Units	Value
Injection Energy	MeV	285
Extraction Energy	MeV	3000
Current at Extraction	A	0.5
Total number of protons in ring	10^{12}	2.52
Beam from Linac		
Pulse Length	ms	0.22
Frequency	MHz	115
Number of Bunches in Pulse		25300
Average Current per Pulse	mA	2
Charge per Pulse	μC	0.44
Number of Protons per Pulse	10^{12}	2.75
Injection Efficiency		0.9
Number of Pulses		1
Timing		
RF Acceleration Time	s	0.12
Pre-booster Cycle Time	s	0.2
Beam profile at Injection		
Acceptance in x (ε_x) (normalized)	π mm · mrad	92
Acceptance in y (ε_y) (normalized)	π mm · mrad	50
Momentum Acceptance (Δp/p)	%	±0.3
Beam profile at Extraction		
Momentum Spread (Δp/p)	%	±0.27
Bunch Length	μs	0.166
Space Charge		
RMS Emittance unnormalized x	mm.mrad	26
RMS Emittance unnormalized y	mm.mrad	14
RMS Emittance unnormalized z	eV.s	0.016
Laslett Tune Shift (after injection)		-0.025
Max Laslett Tune Shift		-0.038
Laslett Tune Shift (at extraction)		-0.006

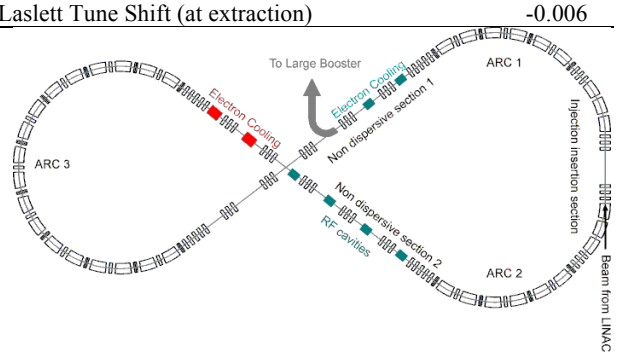

Figure 2: Figure-of-eight ring outline.

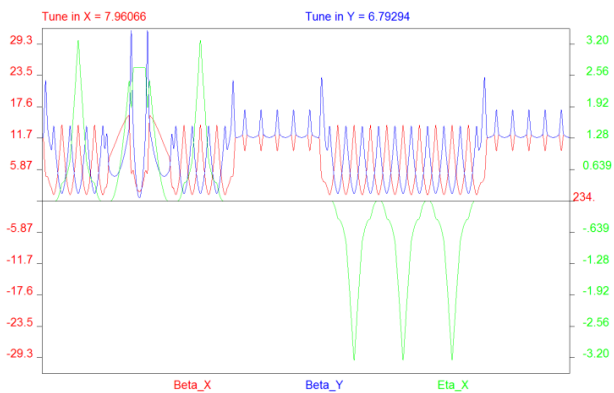

Figure 3: Plot of lattice functions for the full system.

Table 3: Main Parameters of Lead Beams

Parameter	Units	Value
Injection Energy	MeV/u	100
Extraction Energy	MeV/u	670
Charge State of Lead Ions		+67
Current at Extraction	A	0.5
Total Number of Lead Ions	10^{10}	4.5
Beam from Linac		
Pulse Length	ms	0.25
Frequency	MHz	115
Number of Bunches in Pulse		28750
Average Current per Pulse	mA	0.1
Charge per Pulse	μC	0.025
Number of Lead Ions per Pulse	10^{9}	2.4
Injection Efficiency		0.7
Number of Pulses		28
Timing		
Electron Energy (for e^- Cooling)	MeV	[.56,.88]
Electron Cooler Current	A	0.3
Electron Cooler Length	m	3
Transverse Cooling Time	ms	16
Longitudinal Cooling Time	ms	55
RF Acceleration Time	ms	144
Pre-booster Cycle Time	s	3.1
Beam Profile at Injection		
Acceptance in x (ε_x) (normalized)	π mm · mrad	92
Acceptance in y (ε_y) (normalized)	π mm · mrad	50
Momentum Acceptance (Δp/p)	%	±1
Emittance in x (ε_x) (normalized)	π mm · mrad	50
Emittance in y (ε_y) (normalized)	π mm · mrad	25
Momentum Spread (Δp/p)	%	±0.3
Beam Profile after Cooling and Accumulation		
Emittance in x (ε_x) (normalized)	π mm · mrad	20
Emittance in y (ε_y) (normalized)	π mm · mrad	10
Momentum spread (Δp/p)	%	±0.054
Beam Profile at Extraction		
Emittance in x (ε_x) (full, normalized)	π mm · mrad	20
Emittance in y (ε_y) (full, normalized)	π mm · mrad	10
Momentum spread (Δp/p) (95% capture efficiency)	%	±0.21
Bunch Length	μs	0.386
Space Charge		
Laslett Tune Shift (at injection)		-0.16
Max Laslett Tune Shift		-0.3
Laslett Tune Shift (at extraction)		-0.09

SPACE CHARGE STUDIES FOR THE PRE-BOOSTER

A new method for calculating quantities of interest such as tunes, dispersion and resonances from the Taylor map of the system, with an accurate approximation of 2D space charge effects on the beam has been recently developed and implemented in code COSY Infinity [4]. We use this method to study the effect of space charge in the pre-booster. Ten thousand particles of uniform distribution were launched using full admittance of the system and tracked for 400 turns. The figures 4 and 5 show the change in the RMS emittance and beam current as a function of total number of turns for protons and lead ions. As can be seen there is no significant change in beam emittance and current after first 100 turns.

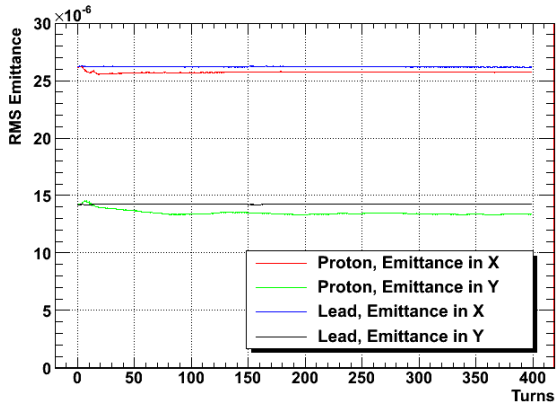

Figure 4: RMS Emittance vs. turns for proton and lead beams due to 2D space charge effects.

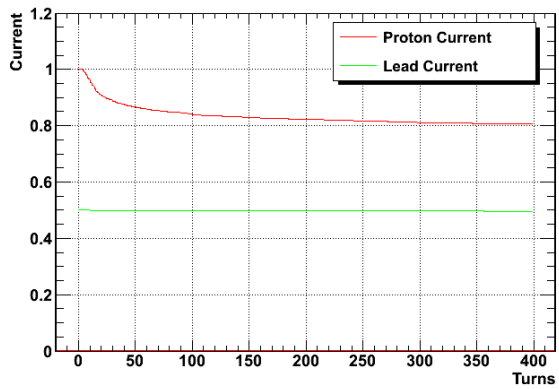

Figure 5: Change in current for proton and lead beams due to 2D space charge effects.

ACKNOWLEDGEMENT

This work was supported by the U.S. Department of Energy, Office of Nuclear Physics, under Contract No. DE-AC02-06CH11357 and grant from Jefferson Lab.

REFERENCES

[1] Afanasev, A. Bogacz, P. Brindza, A. Bruell, L. Cardman, Y. Chao, S. Chattopadhyay, E. Chudakov, P. Degtiarenko, J. Delayen, Ya. Derbenev, R. Ent, P. Evtushenko, A. Freyberger, D. Gaskell, J. Grames, A. Hutton, R. Kazimi, G. Krafft, R. Li, L. Merminga,. *Zeroth–OrderDesign Report for the Electron-Ion Collider at CEBAF*. 2007.

[2] *Advanced Concepts for Electron-Ion Collider*. Derbenev, Y. Paris, France : Proceedings of EPAC 2002, 2002. pp. 314-316.

[3] M. Berz and K. Makino. COSY INFINITY beam physics manual. Technical Report MSUHEP-60804, Department of Physics and Astronomy, Michigan State University, East Lansing, MI 48824, 2006. see also http://cosy.pa.msu.edu.

[4] Method to extract transfer maps in the presence of space charge in charged particle beams, E. Nissen, B. Erdelyi, S. Manikonda : Proceedings of IPAC 2010, 2010. pp. 1967-1969.